Solidification Characteristics and Defect Formation Mechanism of the Fourth Generation Ni-Based Single Crystal Superalloy

Wenchao Yang*, Jun Zhang, Lin Liu
State Key Laboratory of Solidification Processing, Northwestern Polytechnical University, Xi'an 710072, China
*Corresponding address: e-mail: wenchaoyang@nwpu.edu.cn

Abstract: Solidification characteristics and defect formation mechanism of the fourth generation Ni-based single crystal superalloy were systematically investigated. The results indicated that the solidification path of the experimental superalloy during directional solidification was determined as followed: L → γ → β-NiAl → γ′→ (γ+γ′) → TCP. The phase transformation process of the peritecticreaction L + β-NiAl → γ′ of the experimental superalloy during directional solidification had been revealed using the planar interface solidification, and the relaxation of some atoms on the matching planes (110)β and (111)γ′ maximized the atomic matching at the interface, increasing the possibility of peritectic γ′ phase nucleated on primary β-NiAl phase in the peritectic reaction. Finally, it was proposed that it was beneficial to reduce the formation tendency of large-angle grain boundary defects at the platform and reduce the orientation difference of low-angle grain boundaries by controlling secondary dendrite orientation.

Keywords: Ni-based single crystal superalloys; solidification characteristics; secondary dendrite orientation

1 Introduction

Nickel-based single crystal (SX) superalloys are a class of materials extensively used for hot components of turbine engines due to their excellent creep strength, oxidation and hot-corrosion resistance at elevated temperature. The need to continuously improve the performance and efficiency of aircraft and power turbines has driven the development of the successive generations of the nickel-based SX superalloys. Consequently, a large number of refractory elements, such as Re, W, Mo, Ta, and Ru, have been added to further improve the high-temperature mechanical properties of the nickel-based SX superalloy. In particular, as a symbol element in the fourth- and fifth-generation nickel-based SX superalloys, the addition of Ru can greatly improve the microstructural stability and the creep resistance. However, the segregation of high-generation Ru-containing SX superalloys is extremely serious due to the increase of refractory elements, which is more likely to cause casting defects. Therefore, it brings challenges to the composition design and microstructure control of high-generation Ru-containing superalloys [1].

In this paper, the solidification characteristics and solidification microstructures of a fourth-generation Ni-based single crystal superalloy were studied, and the effect of the composition characteristic on the solidification characteristics and solidification microstructures was investigated. Finally, the effects of secondary dendrite orientation on the dendrite growth and orientation evolution within the platforms of simplified blades and solid turbine blades were investigated through a combination of experiment and numerical simulation, and the methods of controlling the stray grain and low-angle grain boundary based on dendrite orientation were further proposed.

2 Experimental procedure

In this work, the nominal composition of the experimental superalloy was as follows (wt.%): 14.0 Co, 6.0 Al, 19.5 (Cr+Mo+W+Ta), 0.1 Hf, 5.4 Re, 3 Ru, and the balance Ni. The single crystal bars with orientation [001] were prepared by liquid metal cooling directionalsolidification furnace. Besides, Singlecrystal blades with different secondary dendrite orientations were prepared byhigh rate solidification furnace. The schematic diagrams of the directional solidification deviceswere shown in Fig. 1.

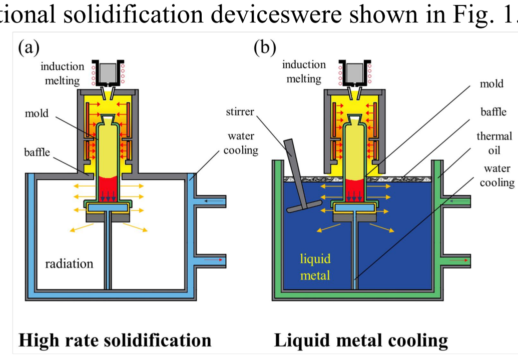

Fig. 1. The schematic of the high rate solidification furnace (a) and liquid metal cooling furnace (b).

3 Result and discussion

Solidification characteristics

Fig. 2 showed the microstructure evolution as a function of the *f*s for the alloy during the planar interface solidification. It could be seen that there were four different microstructure morphologies along the growth direction.The solidification path of the experimental superalloy during directional solidification was determined as followed: L → γ → β-NiAl → γ′→ (γ+γ′) →TCP.

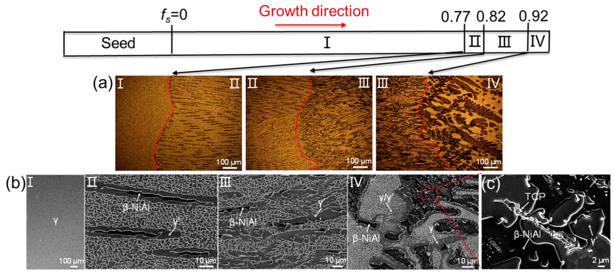

Fig. 2 The microstructure evolution of the alloy at the withdrawal rate of 1 μm/s (a) OM images of the solidification sequence solidified with a planar solid-liquid interface. (b) Higher magnification SEM micrographs of the areas marked as I, II, III, and IV respectively. (c) SEM micrograph showing the area in (b)IV marked by the red dotted rectangle at higher magnification.

The solidification sequence after the solidification of the γ phase was as followed during directional solidification of the experimental superalloy: the primary β-NiAl phase was first precipitated from the liquid directly, and then the coarse γ′ phase was formed by an incomplete peritectic reaction of L + β-NiAl→ γ′ + β-NiAl$_{(Residual)}$.To further reveal the phase transformation mechanism of theperitectic reaction from the crystallographic point of view, TEM observations were performed and the results were shown in Fig. 3. The OR between β-NiAl phase and γ′ phase might be identified as $[001]_\beta$ // $[110]_{\gamma'}$ and $(110)_\beta$ // $(111)_{\gamma'}$. The relaxation of some atoms on the matching planes $(110)_\beta$ and $(111)_{\gamma'}$ maximized the atomic matching at the interface, increasing the possibility of peritectic γ′ phase nucleated on primary β-NiAl phase in the peritectic reaction

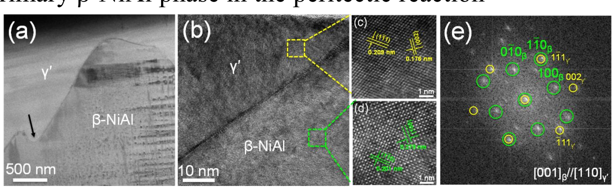

Fig. 3 TEM micrograph and HRTEM analysis of the β-NiAl and γ′ phases. (a) TEM bright-field image. (b) HRTEM image of the two phases and Enlarged HRTEM images showing (c) the γ′ phase and (d) the β-NiAl phase. (e) corresponding FFT image of (b).

Defect formation mechanism

Fig. 4 showed theschematic diagrams of dendrite growth path within the platform base of the blades. The edge B on the bottom surface of the blade platform had the property of being the first to advance to the liquid-line temperature, and the matrix dendrite branching in the leaf body region grew farther into the path of this edge, and the edge B might be the most susceptible to supercooling nucleation at the edge plate to produce stray grains. The formation of stray grainswas determined by the competition between the supercooling time and the growth time of the branching crystals. Changing θ_2 affected the path of the matrix branching crystals in the leaf body region to the edge corner B, which had the greatest tendency to form stray grains in the platform, and this was important for the suppression of the formation of stray grains defects in the platform.

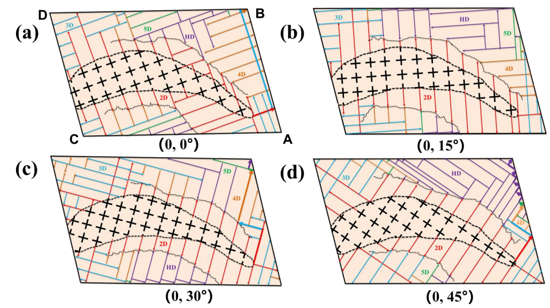

Fig. 4 Schematic diagrams of dendrite growth path within the platform base of blades: (a) θ1=0° andθ2=-2°; (b) θ1=0° and θ2=13°; (c) θ1=0° and θ2=28°; (d) θ1=0° and θ2=45° (The bold arrows showed the paths of dendrite branching from the blade zone growing to the extremity B within the platform base).

Conclusion

1.The results indicated that the solidification path of the experimental superalloy during directional solidification was determined as followed: L → γ → β-NiAl → γ′→ (γ+γ′) →TCP.

2. Controlling the secondary dendrite orientations could effectively inhibit the stray grains and low-angle grain boundaries defects at the blade platform.

Acknowledgments

This work was funded by National Natural Science Foundation of China (51771148, 52071263, 52031012, 52322410), Science Center for Gas Turbine Project (P2021-A-IV-001-001), The Key Research and Development Program of Shaanxi Province (2023-YBGY-432), Natural Science Basic Research Plan in Shaanxi Province of China (2021JC-13) and Research Fund of the State Key Laboratory of Solidification Processing (NPU), China (2021-QZ-03).

References

[1] Z. Shang, X. P. Wei, D. Z. Song, et. al. Microstructure and mechanical properties of a new nickel-based single crystal superalloy. Journal of Materials Research and Technology, 2020, 9(5): 11641-11649.